

REVIEW ARTICLE

Nanotechnology-enabled delivery of NQO1 bioactivatable drugs

Xinpeng Ma*†, Zachary R. Moore*, Gang Huang, Xiumei Huang, David A. Boothman, and Jinming Gao

Department of Pharmacology, Simmons Comprehensive Cancer Center, University of Texas Southwestern Medical Center, Dallas, TX, USA

Abstract

Current cancer chemotherapy lacks specificity and is limited by undesirable toxic side-effects, as well as a high rate of recurrence. Nanotechnology has the potential to offer paradigm-shifting solutions to improve the outcome of cancer diagnosis and therapy. β -Lapachone (β -lap) is a novel anticancer agent whose mechanism of action is highly dependent on NAD(P)H:quinone oxidoreductase 1 (NQO1), a phase II detoxifying enzyme overexpressed in solid tumors from a variety of cancer types. However, the poor water solubility of β -lap limits its clinical potential. A series of drug formulations were developed for systemic administration in preclinical evaluations. Encapsulation of β -lap into polymeric micelles showed less side-effects and higher maximum tolerated dose (MTD), prolonged blood circulation time and preferential accumulation in tumors with greatly improved safety and antitumor efficacy. The prodrug strategy of β -lap further decreases the crystallization of β -lap by introducing esterase degradable side chains to the rigid fused ring structure. β -Lap prodrugs considerably increased the stability, drug-loading content and delivery efficiency of nanoparticles. The optimized formulation of β -lap-dC₃ prodrug micelles showed excellent antitumor efficacy in treating orthotopic non-small cell lung tumors that overexpress NQO1, with target validation using pharmacodynamic endpoints.

Keywords

Cancer targeting, drug delivery, β -lapachone, nanoparticle, NQO1, prodrug

History

Received 22 May 2015
Revised 6 July 2015
Accepted 13 July 2015
Published online 5 October 2015

Introduction

There is a paramount need for broad-spectrum, yet cancer-specific therapies. Targeted therapies directed against proliferative differences between tumor and normal cells have been exhausted, and their off-target effects on healthy tissues typically result in substantial toxicities that limit treatment dose, duration and efficacy. More than a decade into the era of ‘‘targeted therapy’’, few cancers are truly amenable to this approach. The successes of molecular targeted therapy – imatinib for chronic myeloid leukemia, erlotinib for epidermal growth factor receptor mutated non-small cell lung cancer (NSCLC), and trastuzumab for human epidermal growth factor receptor-2-positive breast cancer – account for only 5% of the 1.7 million cancer cases in the USA annually [1]. Furthermore, these targeted approaches suffer from acquired resistance after prolonged treatment.

Currently, nanomedicine, or the use of nanoscale (10–200 nm) constructs for therapeutic delivery, is emerging as a powerful tool in cancer care [2–4]. Advances in nanomaterials and nanotechnology have paved the way for several carriers,

such as liposomes [5], dendrimers [6] and polymeric micelles [7,8]. Polymeric micelles are supramolecular core-shell nanoparticles composed of amphiphilic block-copolymers. Advantages afforded for drug delivery include the presence of a hydrophobic inner core for drug entrapment, as well as a hydrophilic outer shell that prevents particle aggregation and opsonization [9,10]. This architecture reduces uptake by the reticuloendothelial system (RES), which prolongs blood circulation time and allows for preferential accumulation in tumor tissue through the enhanced permeability and retention (EPR) effect [11,12]. Genexol™, a polymeric micelle formulation for the delivery of paclitaxel, has recently been approved in South Korea (Phase III trials in the USA) for cancer treatment with considerably reduced clinical toxicity (e.g. hypersensitivity reactions) compared to Cremophor in Taxol®. DTXL-TNP, a targeted polymeric nanoparticle containing chemotherapeutic docetaxol (DTXL) was recently developed in clinical translation by BIND Therapeutics Inc., has exhibited markedly enhanced tumor accumulation at 12 h and prolonged tumor growth suppression compared to solvent-based DTXL formulation [7]. These advances illustrate the emerging importance of nanotechnology and drug delivery for the safe and efficacious treatment of cancer.

NQO1, an exploitable biomarker in solid tumors

NADPH:quinone oxidoreductase 1 (NQO1) is a phase II detoxifying enzyme that catalyzes the two-electron

*These authors contributed equally to this article.

†Present address: BIND Therapeutics, Inc., 325 Vassar Street, Cambridge, MA 02139, USA.

Address for correspondence: David A. Boothman and Jinming Gao, Department of Pharmacology, Simmons Comprehensive Cancer Center, University of Texas Southwestern Medical Center, 6001 Forest Park Road, Dallas, TX 75390-8807, USA. E-mail: David.Boothman@UTSouthwestern.edu (D. A. Boothman); Jinming.Gao@UTSouthwestern.edu (J. Gao)

oxidoreduction of target quinones to promote their neutralization and removal from the cell [13]. Both endogenous and exogenous quinones can generate toxic reactive oxygen species (ROS) that damage DNA, proteins and lipids. Reduction by NQO1 generates a hydroquinone from the parent quinone that is typically much more stable and can be conjugated by other phase II enzymes for cellular export [14].

The kinetic mechanism of this two-electron reduction is called ‘‘Ping-Pong Bi Bi’’ [15]: NADH or NADPH (either can be used with equal efficiency) first binds NQO1 and reduces its FAD cofactor, NAD^+ or NADP^+ is released, and finally the quinone binds and is reduced in one step to the hydroquinone [16]. The active site of NQO1 is a flexible hydrophobic pocket that can accommodate consecutive binding of NADH/NADPH and a variety of quinones with a diversity of structures [17,18]. Dicoumarol, a vitamin K analog, is a potent inhibitor of NQO1 and binds tightly in the active site to the oxidized form of the enzyme [16].

Interest in NQO1 was sparked by the discovery that it is overexpressed in solid tumors from a variety of cancer types [19–21]. NQO1 is markedly overexpressed in non-small cell lung cancer (NSCLC), breast, colon and prostate cancers [22,23]. Up to 90% of pancreatic cancer cases exhibit 12-fold overexpression of NQO1 on average [24]. Reports on NQO1 often focus on its potential use as a biomarker that could aid diagnosis, since it appears to be overexpressed very early in cancer progression, and even in precancerous lesions [21]. The mechanism of NQO1 overexpression in solid tumors is still not fully understood, and likely varies depending on the molecular context in each individual cancer type. For example, frequent mutations in NSCLC disrupt the KEAP1-Nrf2 interaction and drive NQO1 expression, whereas in pancreatic ductal adenocarcinoma (PDA), K-ras mutations increase Jun dimerization with Nrf2 to promote transcription of NQO1 [25,26].

β -Lapachone, an NQO1-bioactivated therapeutic

β -Lapachone (β -lap) was the first therapeutic compound found to have a mechanism of action dependent on an NQO1 catalyzed futile cycle. Originally, β -lap was isolated from the bark of the Pink Lapacho tree (*Handroanthus impetiginosus*), and exhibited anti-trypanosomal and anti-bacterial properties [27,28]. Later, it was discovered to cause lethality to cancer cells, especially when combined with DNA damaging agents like ionizing radiation (IR), but the mechanism was hypothesized to be DNA damage repair inhibition, which is now known to be a secondary effect of its primary mechanism [29]. It was not until treatment times were reduced from 24 h and longer to 2–4 h that the NQO1 specificity of β -lap was finally elucidated [30].

β -Lap is a 1,2 naphthoquinone substrate for NQO1, which catalyzes a 2-electron reduction. What makes β -lap unique compared to other quinones that are neutralized by NQO1 is that the resulting hydroquinone form of β -lap is exceptionally unstable. Instead of being conjugated and removed from the cell, the hydroquinone form of β -lap spontaneously reacts with oxygen in two steps: first, an oxidation to the semiquinone form, and second, a reversion back to the parent quinone. Each of the spontaneous oxidation steps

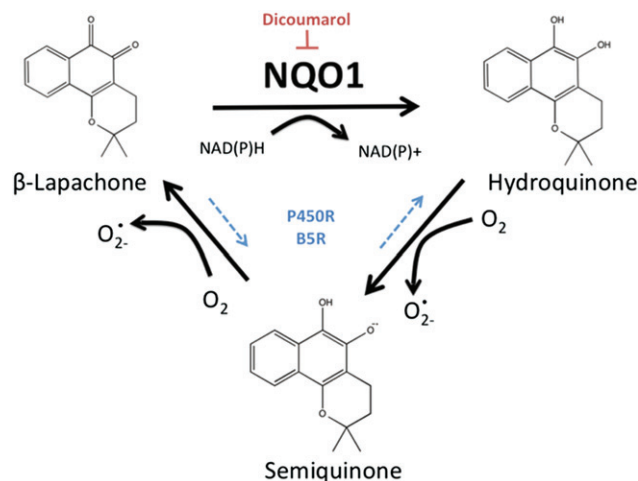


Figure 1. Futile redox cycle of β -lap by the two-electron oxidoreductase, NQO1. NQO1 oxidizes NADPH or NADH to reduce β -lap to a hydroquinone, which spontaneously reacts with oxygen to revert to the parent compound through the semiquinone intermediate. p450R and b5R catalyze the less efficient one-electron oxidoreductions. Dicoumarol is a competitive NQO1 inhibitor.

generates a superoxide anion radical. In sum, these reactions form a futile redox cycle in which β -lap is converted to a hydroquinone by NQO1, oxidizing NADH and NADPH, and the hydroquinone reverts back to β -lap, generating superoxide (Figure 1) [30]. This cycle occurs very rapidly in cells that express NQO1; 1 mol of β -lap can cause 60 mol of NAD(P)H to be consumed and 120 mol of free radicals to be generated in less than 10 min [30]. Furthermore, β -lap toxicity is completely dependent on NQO1 activity, as it is blocked by inhibition of NQO1 with dicoumarol or with RNAi-mediated knockdown of NQO1 expression [31,32].

Rapid generation of superoxide and consumption of NAD(P)H are potentially destructive to NQO1-overexpressing cells that are treated with β -lap. The superoxide radicals generated directly from the futile cycle are reactive and short lived, but they are converted to other more stable ROS, including hydrogen peroxide. These reactions are catalyzed by manganese superoxide dismutase and spontaneous chemical processes. Hydrogen peroxide is membrane permeable and has a 1000-fold longer half-life than the superoxide anion, allowing it to diffuse from the cytoplasm (where the NQO1-mediated futile cycle occurs) to the nucleus, where it is then converted back to superoxide through the Fenton reaction and reacts with DNA [33,34]. The DNA damage caused by β -lap consists of single strand breaks and base oxidation, with a notable lack of double-strand breaks compared to IR [35].

β -Lap induces apoptosis-like cell death in cancer cells that overexpress NQO1 as a result of two primary causes: a rapid burst of DNA damage that exceeds the repair capacity of the cell, and acute energy depletion resulting from the loss of NADP(H) and NAD^+ , caused by both the redox futile cycle and PARP1 hyperactivation. PARP1 attempts to repair the DNA single strand break by binding to the sites of damage and catalyzing the poly(ADP ribosylation) of target DNA repair proteins to recruit and activate them [36,37]. However, due to the large number of lesions rapidly caused by β -lap treatment, PARP1 is overwhelmed and completely consumes

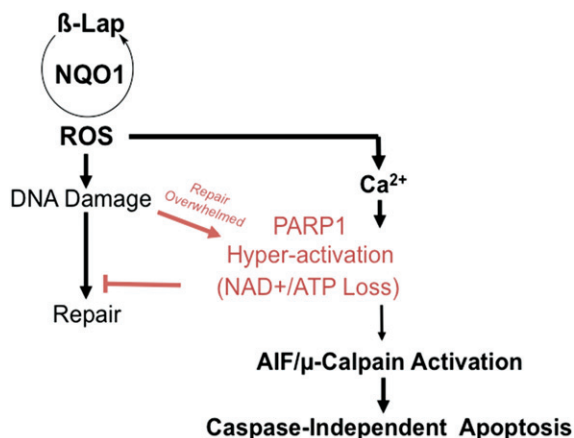


Figure 2. Cell death induced by the NQO1 bioactivatable drug, β -lapachone. The NQO1-mediated futile cycle generates ROS, which causes DNA single strand breaks and base damage that hyperactivates PARP1. PARP1 hyperactivation results in rapid NAD^+ and ATP depletion, AIF and μ -Calpain activation by Ca^{2+} release from the ER into the cytoplasm, and cell death by a caspase-independent NAD^+ -Keresis mechanism.

the available pool of NAD^+ , which has been supplemented by the oxidation of NADH in the futile cycle, to form long chains of poly(ADP ribose) (PAR) [38]. β -Lap treatment is also associated with release of calcium from the endoplasmic reticulum and the subsequent activation of μ -Calpain [39,40]. Much like members of the caspase family, μ -calpain is a cysteine protease that initiates cell death through cleavage of target proteins, including PARP1 [41]. Apoptosis inducing factor (AIF) translocates from the mitochondrial membrane to the nucleus and contributes to chromatin condensation, DNA fragmentation, and death [42,43]. The result is cell death with the following characteristics: PAR formation, ATP and NAD^+ depletion, caspase independence, μ -calpain cleavage, atypical PARP1 cleavage and TUNEL staining [38,41,44,45]. The sequence of this cell death process is depicted in Figure 2, and the primary driver of this form of cell death, called NAD^+ -Keresis, is depletion of NAD^+ and ATP secondary to PARP1 hyperactivation. Cell death exhibiting similar biomarkers is observed in other contexts, including glutamine excitotoxicity in neurons, and ischemia reperfusion in neurons and heart tissue, with increased reliance on PAR signaling occurring in some cases [46,47]. Though there are other reports about cell death after β -lap treatment occurring through caspase-dependent apoptosis, this has only been observed after long-term treatment (8–74 h versus 2–4 h), which likely occurs through a different mechanism, since NQO1 dependence is also reduced with these longer treatment times [48,49].

Development of drug delivery strategies to overcome β -lap limitations

Overexpression of NQO1 in cancer cells makes β -lap a useful candidate for tumor-selective drug therapy with reduced toxicities to healthy cells/tissue that lack or express low levels of the enzyme. Despite the potency and selectivity of β -lap in killing NQO1-containing cancer cells *in vitro*, the low water solubility of β -lap (0.038 mg/mL or 0.16 mM) limits its application *in vivo*. To overcome the solubility and

bioavailability challenges, we developed a series of drug formulations for systemic administration in preclinical evaluations.

Hydroxylpropyl- β -cyclodextrin (HP β CD) increases the solubility of β -lap

Cyclodextrins (CDs) are a well-known class of host molecules that can form inclusion complexes with a variety of drugs to improve drug solubility, stability, as well as bioavailability [50,51]. CDs consist of different number of glucopyranose units that are connected by glycosidic linkages. The shape of these molecules is similar to a truncated cone, which has a hydrophilic outer surface and a hydrophobic inner cavity. We screened four different types of CDs: α -CD, β -CD, HP β CD and γ -CD whose inner diameters of the hydrophobic cavity are approximately 4.7–5.3, 6.0–6.5, 6.0–6.5 and 7.5–8.3 Å, respectively.

β -CD and HP β CD, a propylene oxide modified β -CD, showed higher association constants with β -lap due to its appropriate cavity size. The maximal solubility of β -lap in HP β CD solution reached 66 mM or 16 mg/mL, over 400-fold increase over β -lap aqueous solubility (0.16 mM) [52]. The host-guest chemistry between HP β CD and β -lap was further confirmed by NMR spectroscopy. The significant nuclear overhauser effect enhancement of the protons located inside the HP β CD cavity was observed with the selective excitation of the methyl protons from β -lap. This result confirmed that the methyl moiety of β -lap is bound inside the cavity and also suggested that HP β CD forms a 1:1 inclusion complex with β -lap. The chemical shift changes of β -lap and HP β CD in the ^1H NMR spectra and the change in fluorescence intensity and maximum emission wavelength of guest β -lap compound by addition of CDs further confirmed the formation of inclusion complexes between these two compounds. Cytotoxicity assays indicated few differences in biologic activity between β -lap and β -lap-HP β CD inclusion complexes, with nearly identical cell responses (cell death in induced apoptosis) and TD_{50} (the toxic dose that kills 50% of the cell population) values (2.1 μM). Subsequently, studies of morbidity and mortality in C57Blk/6 mice suggested a LD_{50} of 50–60 mg/kg, with no morbidity or mortality following 20–50 mg/kg β -lap in HP β CD inclusion complex. Complexation of β -lap with HP β CD offers a major advancement in improvement of bioavailability of this very active anticancer agent. However, the clinical form of β -lap-HP β CD complex (ARQ 501) underwent unsuccessful clinical trials in patients with several different cancer types. The reason for failure includes dose-limiting toxicity in the form of hemolytic anemia due to HP β CD, nonspecific drug distribution [53], resulting in limited antitumor efficacy, and choice of tumors not known to over-express NQO1.

β -Lap-containing micelles increases the safety and antitumor efficacy of β -lap

Clinical limitation of the β -lap-HP β CD complex indicated the need for a more effective delivery vehicle. Nanomedicine systems can take advantage of the leaky tumor vasculature also known as the EPR effect for accumulation in the tumor tissues [11,12]. Polymer micelles have a unique core-shell

structure as a result of the self-assembly of amphiphilic block copolymers in the aqueous environments. The hydrophobic core acts as a solubilizing reservoir for water insoluble drugs [54], providing protection from enzymatic degradation and inactivation [55]. The hydrophilic micellar corona, in turn, forms a hydrating layer on the surface of the micelle that hinders plasma protein adsorption and subsequent rapid phagocytic clearance by the RES [56]. Early work by Langer and coworkers provided the first example for the use of stealth micelles in the delivery of hydrophobic lidocaine drugs with greatly improved safety and biological efficacy, which paved the way for the use of this nanoconstructs for drug delivery applications [9].

We attempted to load β -lap into poly(ethylene glycol)-*b*-poly(D,L-lactic acid) (PEG-PLA, MW 10 000 Da) polymer micelles [3]. Several different micelle fabrication techniques (film sonication, solvent evaporation and dialysis) were examined with the purpose of generating β -lap micelles with a small size, high yield, and adequate drug-loading density and efficiency. The film sonication method produced the highest β -lap loading of micelles among all the three fabrication methods, with a $4.7 \pm 1.0\%$ drug loading at a theoretical loading of 10%, a loading efficiency of $41.9 \pm 5.6\%$. The *in vitro* release kinetics of β -lap from PEG-PLA polymer micelles showed that the time for 50% of drug release ($t_{1/2}$) is 18 h, with the majority of the drug ($\sim 75\%$) being released over the course of 4 days. Using three different cancer cell lines, β -lap micelle treatment showed a substantial increase in cytotoxicity in NQO1+ cells over NQO1- cells, highlighting the system as a potential treatment strategy against NQO1-overexpressing tumors. Prior clinical trial data revealed the dose-limiting toxicity (e.g. hemolytic anemia) of ARQ 501 [53]. The hemolytic data of different β -lap formulations show that β -lap-HP β -CD indeed caused hemolysis, with concentrations at 1.0 and 1.5 mg/mL β -lap resulting in $47 \pm 1\%$ and $52 \pm 2\%$ hemolysis, respectively. No measurable hemolysis was observed from β -lap micelles at all concentrations examined. Morbidity and mortality responses of β -lap micelle and β -lap-HP β -CD in healthy mice at different doses also confirmed the safety of β -lap micelles. Five i.v. injections every other day of 30 mg/kg β -lap-HP β -CD resulted in no deaths with moderate side effects, like labored breathing and an irregular gait. These symptoms were more intense at higher doses of 40 and 50 mg/kg β -lap-HP β -CD, yielding severe muscle contractions, labored breathing, and lethality in some cases. In contrast, β -lap micelle doses ranging from 30 to 50 mg/kg did not result in any deaths and had significantly less side effects. Mice injected with 40 and 50 mg/kg of β -lap micelles experienced mild and moderate labored breathing and irregular gait [3].

Pharmacokinetic data showed that β -lap micelles had a distribution phase half-life ($t_{1/2,\alpha}$) of 2 h, and an elimination half-life ($t_{1/2,\beta}$) of 28 h (Figure 3A), much longer than ARQ501 ($t_{1/2,\beta} = 24$ min). β -Lap micelles were preferentially distributed in tumors ($\sim 1.5\%$ injected dose/g tissue, Figure 3B), which are higher than those in heart, lungs and muscles. Liver and spleen showed high uptake of β -lap micelles (5.8% and 3.4% ID/g, respectively). However, no chronic toxicity was observed in these tissues 3 months after the treatment, which was attributed to their low NQO1

expression and high catalase levels [42]. β -Lap micelles showed significantly improved antitumor efficacy than β -lap-HP β -CD complex. In mice bearing subcutaneous A549 lung tumors, a 30 mg/kg dose of β -lap-HP β -CD proved rather ineffective at suppressing tumor growth (Figure 3C and D), with only a slight improvement over the HP β -CD vehicle control. Improved antitumor efficacy was noted at 40 mg/kg β -lap-HP β -CD, especially at earlier times of tumor growth. In contrast to β -lap-HP β -CD, all doses of β -lap micelles (30, 40 and 50 mg/kg) suppressed A549 NSCLC tumor growth from days 1 to 9 (Figure 3E). Animals receiving 50 mg/kg β -lap micelles resulted in the greatest efficacy and tumor regression, with tumors at days 14 and 21 measuring 170 ± 83 and 152 ± 110 mm³, respectively. At this dose, β -lap micelles showed superior antitumor efficacy and significantly improved survival versus vehicle control ($p = 0.01$), with no lethality observed >100 days after treatment (Figure 3F). Histological analyses of various organs from long-term surviving mice treated with β -lap micelles showed no toxicity. In addition to the subcutaneous A549 tumors, β -lap micelles have also shown significantly improved antitumor efficacy and survival in mice bearing orthotopic Lewis lung carcinoma [3].

Esterase-activatable β -lap prodrug micelles further improves formulation, safety and efficacy

The concept of developing β -lapachone prodrugs began with the development of Schiff-base β -lapachone derivatives [57]. One limitation of the β -lap/PEG-*b*-PLA micelles was the lack of micelle stability. Upon overnight storage at room temperature, β -lap was found to form yellow needle crystals from the micelles, leading to reduced drug loading density (e.g. 2.2%) [2]. To overcome the formulation challenge, we recently adopted a prodrug strategy to improve the micelle stability and formulation properties of β -lap [58]. Prodrugs have been widely used in pharmaceutical industry to improve the physicochemical and biopharmaceutical properties of parent drugs [59]. Among these, ester groups are most commonly used to improve lipophilicity and membrane permeability of drugs containing carboxylate or phosphate groups [60]. Ester groups are readily hydrolyzed by many types of esterase and convert inactive prodrugs into active parental drugs in the body.

We first evaluated the monoester derivative of β -lap (mC₆ was used as an example). Although mC₆ formed micelles with relatively high drug loading efficiency, it is too hydrolytically active (aided by the neighboring hydroxyl group) resulting in unstable micelle composition during storage in the PBS buffer (50% conversion after 2 days at 4 °C). Consequently, we developed diester derivatives of β -lap for micelle loading. Diester prodrugs were synthesized at higher temperature (110 °C) from fatty acid anhydrides using zinc powder as the reducing agent [61]. For anhydrides with shorter chain lengths (i.e. C₂-C₆), over 80% yields were obtained (Figure 4A). For β -lap-dC₁₀ and β -lap-dC₁₆ prodrugs (abbreviated to dC_n in subsequent names), yields decreased to 42% and 14%, respectively. All diester prodrugs were hydrolytically stable in PBS.

After prodrug preparation, we performed drug-loading studies in PEG-PLA micelles (M_n = 10 kD with 5 kD for the

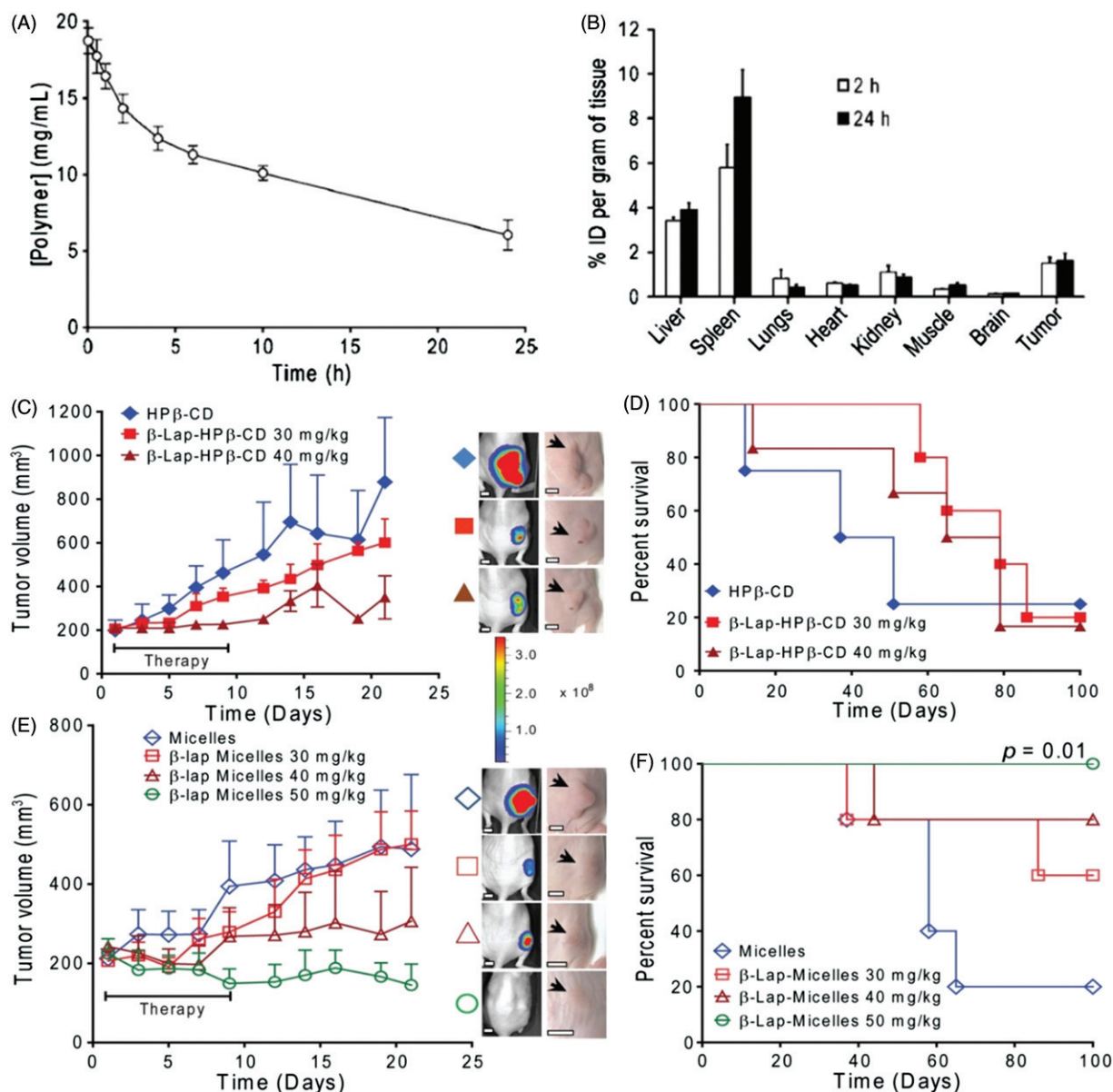
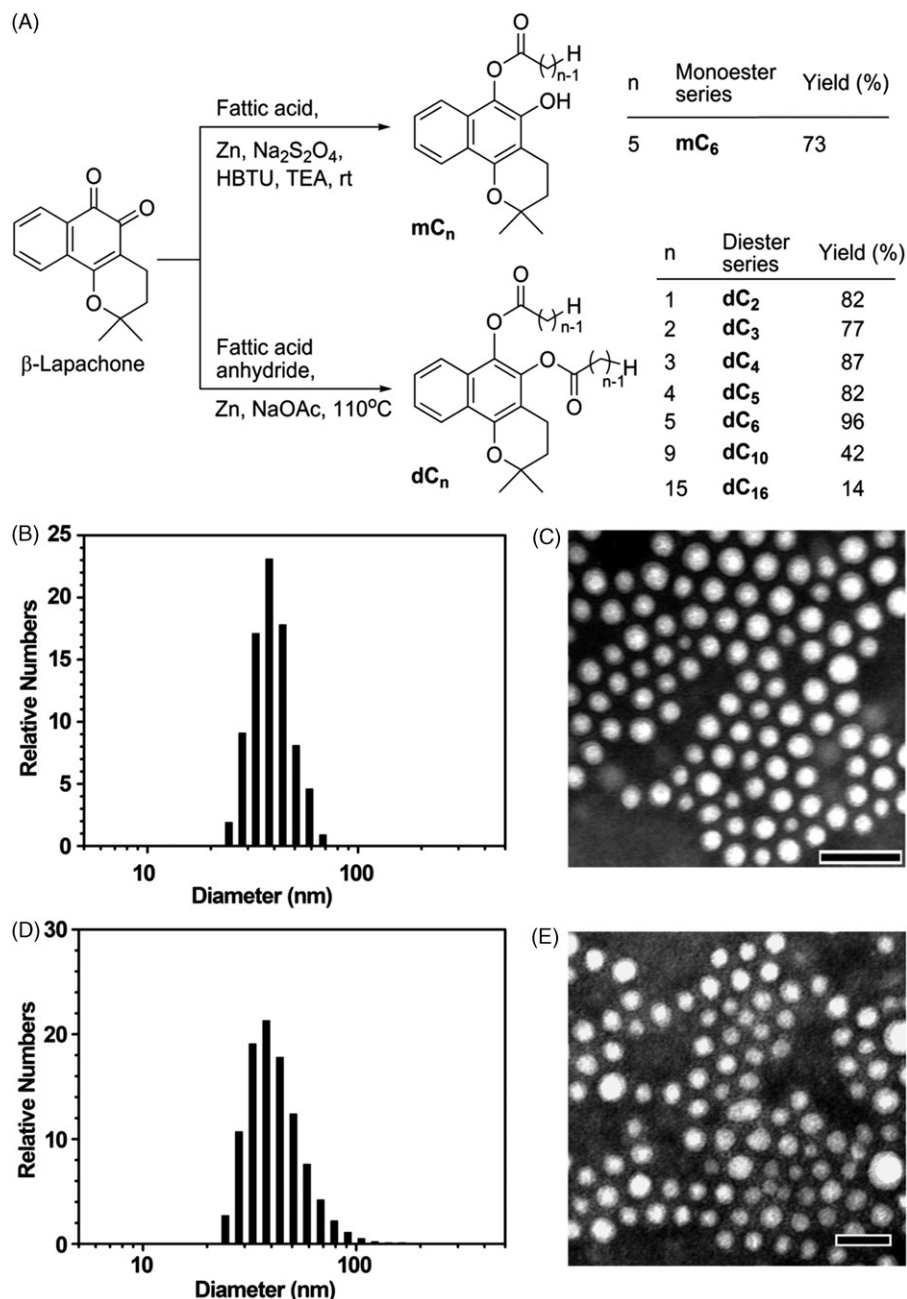


Figure 3. Pharmacokinetic analysis of β -lap polymer micelles (40 mg/kg) and evaluation of antitumor efficacy of β -lap micelles in female athymic nude mice bearing subcutaneous A549 NSCLC xenografts. (A) Blood concentration of β -lap micelles as a function of time. Pharmacokinetic parameters (e.g. $t_{1/2}$) were calculated using a two-compartment pharmacokinetic model [26]. (B) Tissue distribution of β -lap micelles in various organs and tissues at 2 and 24 h after i.v. administration. (C) Tumor growth inhibition and (D) Kaplan–Meier survival curve of mice bearing subcutaneous A549 xenografts after 30 or 40 mg/kg β -lap-HP β -CD or HP β -CD vehicle alone used as a negative control. (E) Tumor growth inhibition and (F) Kaplan–Meier survival curve of mice bearing subcutaneous A549 NSCLC xenografts after 30–50 mg/kg β -lap micelles. PEG-PLA micelle alone was used as a negative control. For all treatment groups, i.v. administering e.o.d. was performed for 9 days. Error bars represent (SE) from three experiments with 5 mice/group. Reproduced with permission from Ref. [3].

PEG and PLA blocks). We compared micelle properties from two formulation methods, solvent evaporation versus film hydration. For β -lap-dC₂, neither method allowed formation of stable, high drug loading micelles because of its fast crystallization rate in water (similar to β -lap). Other diester derivatives were able to form stable micelles with high drug loading. We chose dC₃ and dC₆ for detailed analyses. The solvent evaporation method was able to load dC₃ and dC₆ in micelles at 79% and 100% loading efficiency, respectively. The apparent solubility of β -lap (converted from prodrug) is 4.1 and 4.9 mg/mL for dC₃ and dC₆ micelles (dC₃M and dC₆M), respectively. At these concentrations, micelle sizes (40–130 nm range) appeared larger than those fabricated

using the film hydration method (30–70 nm) and moreover, the dC₃ micelles from solvent evaporation were stable for only 12 h at 4 °C. In comparison, the film hydration method allowed for a more efficient drug loading (>95% loading efficiency), larger apparent solubility (>7 mg/mL) and higher stability (>48 h) for both prodrugs. Close comparison between dC₃M and dC₆M showed that dC₃M had smaller average diameters (30–40 nm) and a narrower size distribution compared to dC₆M (40–70 nm) by dynamic light scattering (DLS) analyses (Figures 4B and 2D). This was further corroborated by transmission electron microscopy that illustrated spherical morphology for both micelle formulations (Figures 4C and 2F).

Figure 4. Syntheses of β -lap prodrugs and the characterization of prodrug loaded micelles. (A) Synthesis of monoester and diester derivatives of β -lap. (B, D) Size distribution histograms of dC_3 (B) or dC_6 micelles (D) from DLS analyses. TEM images of dC_3 (C) or dC_6 micelles (E) showing spherical morphologies of prodrug micelles (scale bars = 100 nm). All micelles in B–E were made from the film hydration method. Reproduced with permission from Ref. [57].



Several reports indicated that tumors of the lung, colon and liver had high esterase expressions and could be exploited for selective drug conversion using an ester prodrug strategy [62,63]. Porcine liver esterase (PLE) was selected as a model enzyme to test the feasibility of conversion of micelle-delivered prodrugs for our *in vitro* studies. At 1 U/mL PLE, dC_3 and dC_6 prodrugs were readily converted to β -lap inside the micelles by PLE. Without PLE, both micelles were stable without detectable prodrug conversion in the PBS buffer (pH 7.4) over 7 days. After prodrug conversion, release of parent drug (i.e. β -lap) from dC_6M had slower release kinetics from micelles than dC_3M where 50% of β -lap was released ($t_{1/2,r}$) from dC_3M and dC_6M at 7.9 ± 0.5 and >48 h, respectively. In cell culture experiments, both dC_3 and dC_6 micelles induced NAD^+ -Keresis similar to β -lap in the presence of PLE [64].

Safety studies showed that dC_3M and dC_6M were 3.5- to >5 -fold more tolerated *in vivo* than β -lap in NOD-SCID mice (i.e. 70 and >100 mg/kg, respectively, versus 20 mg/kg β -lap-HP β CD), respectively. At MTD of prodrug micelles, mice showed less severe reactions than what are typically noted with β -lap-HP β CD. Mice exposed to β -lap-HP β CD had severe reactions immediately after treatment that dissipated 30–45 min after injection and were not associated with weight loss or toxicities to normal tissues [3,45,65]. UV-vis spectroscopy analyses of mouse red blood cells found only negligible hemolysis by dC_3M and dC_6M compared to treatment with β -lap-HP β CD at the same concentration of 2 mg/mL β -lap ($<5\%$ versus $>50\%$, respectively). In addition to hemolysis, β -lap-HP β CD also caused methemoglobinemia (MH), where it reacts with hemoglobin, causing iron oxidation (Fe^{2+} to Fe^{3+} , 628 nm) [66]. In contrast, exposure of

mouse red blood cells to dC₃ or dC₆ micelles did not show observable MH. These results further support the stealth effect of PEGylated micelles and the enhanced safety of β -lap prodrug micelles by avoiding drug exposure to mouse plasma.

The antitumor efficacy of dC₃M or dC₆M was performed in female NOD-SCID mice bearing orthotopic fire-fly luciferase-transfected A549 tumors. Quantitative analyses of BLI intensities showed that treatment with dC₃M resulted in obvious tumor suppression, especially at higher doses of dC₃M (50 and 70 mg/kg) [64]. Changes in tumor volumes (monitored by BLI intensity) in the control group and dC₆M showed rapid tumor growth at day 35. In the long-term survival assessments, 50% of control animals treated with blank micelles died at day 88, and treatment of mice with dC₆M did not show any significantly increased survival benefit. In contrast, dC₃M showed significantly increased antitumor efficacy at all doses tested. At 30 mg/kg dC₃M, the average 50% survival time was 108 days, statistically similar to the average survival of mice exposed to β -lap-HP β CD (ARQ501, 25 mg/kg) at 104 days. The medium survival times for tumor-bearing mice treated with 50 or 70 mg/kg dC₃M were significantly longer at 115 and 139 days, respectively. It is worth noting that 20% of the 70 mg/kg dC₃M-treated mice were still alive (“apparently cured”) even after 250 days (not graphed) and remained disease free at the time of reporting these data. Kaplan–Meier survival curves indicated a statistically significant survival advantage of 70 mg/kg dC₃M over blank micelle carrier alone ($p \leq 0.0004$) or β -lap-HP β CD ($p \leq 0.008$). PARP-1 hyperactivation further supported the high antitumor efficacy of dC₃M. The dC₃M treatment induced significant PARP-1 hyperactivation as early as 15 min and lasted for 180 min. β -Lap-HP β CD caused less PARP-1 hyperactivation and stopped at 120 min. In contrast, dC₆M stimulated negligible PARP-1 formation in 120 min and adjacent normal tissue showed no PARP-1 hyperactivation. The ATP loss of tumor tissue treated with dC₃M or β -lap-HP β CD was coincident with their PARP1 formation. The ATP level of tumor tissue treated with β -lap-HP β CD reached a minimum at 90 min and showed some recovery at 120 min, while dC₃M still took effect at this time [64]. These results also illustrate the value of pharmacodynamic endpoints as early biomarkers to predict antitumor response in drug delivery systems where pharmacokinetic analysis may not be able to differentiate bioavailable drugs from encapsulated drugs.

Summary

β -Lap is a promising anticancer drug with a unique NQO1-specific death mechanism. However, the poor water solubility of β -lap limits its clinical potential. Early formulation of β -lap-HP β CD showed a >400-fold increase in solubility, but underwent unsuccessful clinical trials in a variety of cancers. The reasons for the failure are fast β -lap clearance from the blood, low distribution in tumors and dose-limiting toxicity from the ARQ 501 formulation. The novel β -lap micelles showed fewer side-effects and higher MTD, prolonged blood circulation time and preferential accumulation in tumor. Therefore, β -lap micelles showed greatly improved safety and antitumor efficacy than β -lap-HP β CD complex in NSCLC

and LLC. The bottleneck for the β -lap micelles is the low drug loading content as a result of low stability due to the crystallization of β -lap from the micelles. The prodrug strategy of β -lap decreases the crystallization of β -lap by introducing esterase degradable side chains to the rigid fused ring structure. β -Lap prodrugs considerably increased the stability, drug loading content and delivery efficiency of nanoparticles. The optimized formulation of dC₃ prodrug micelles showed excellent antitumor efficacy in treating orthotopic NSCLC tumors that overexpress NQO1, with target validation in pharmacodynamic endpoints. The advantages of high loading content, ease of scale-up, low toxicity and broader therapeutic window, suggest that dC₃ prodrug micelles are feasible for clinical evaluation.

For clinical translation, the tumor-specific DNA damage caused by β -lap or β -lap prodrug micelles can be further exploited in different combination therapy settings. For example, β -lap can be combined with low doses of IR to yield much greater efficacy [67,68]. Other chemotherapeutic agents that prevent the repair of DNA damage (e.g. DNA repair inhibitors) may also be combined for synergistic effects with added tumor specificity in combination with β -lap [69,70]. These combination treatments help advance the application of β -lap in clinical evaluation, but a thorough examination of potential treatment strategies is necessary to improve the efficacy of NQO1-bioactivated drugs at low doses.

Declaration of interest

The authors report no declarations of interest. This research was supported by NIH/NCI R01 CA102972 and CPRIT RP120897 to D.A.B. and J.G.

References

1. Siegel RL, Miller KD, Jemal A. Cancer statistics, 2015. *CA Cancer J Clin* 2015;65:5–29.
2. Blanco E, Bey EA, Dong Y, et al. β -Lapachone-containing PEG-PLA polymer micelles as novel nanotherapeutics against NQO1-overexpressing tumor cells. *J Control Release* 2007;122:365–74.
3. Blanco E, Bey EA, Khemtong C, et al. β -Lapachone micellar nanotherapeutics for non-small cell lung cancer therapy. *Cancer Res* 2010;70:3896–904.
4. Blanco E, Kessinger CW, Sumer BD, Gao J. Multifunctional micellar nanomedicine for cancer therapy. *Exp Biol Med* (Maywood) 2009;234:123–31.
5. Allen TM, Cullis PR. Liposomal drug delivery systems: from concept to clinical applications. *Adv Drug Deliv Rev* 2013;65:36–48.
6. Kesharwani P, Jain K, Jain NK. Dendrimer as nanocarrier for drug delivery. *Prog Polym Sci* 2014;39:268–307.
7. Hrkach J, Von Hoff D, Mukkaram Ali M, et al. Preclinical development and clinical translation of a PSMA-targeted docetaxel nanoparticle with a differentiated pharmacological profile. *Sci Transl Med* 2012;4:128ra39.
8. Sutton D, Nasongkla N, Blanco E, Gao J. Functionalized micellar systems for cancer targeted drug delivery. *Pharm Res* 2007;24:1029–46.
9. Gref R, Minamitake Y, Peracchia MT, et al. Biodegradable long-circulating polymeric nanospheres. *Science* 1994;263:1600–3.
10. Torchilin VP. Structure and design of polymeric surfactant-based drug delivery systems. *J Control Release* 2001;73:137–72.
11. Hashizume H, Baluk P, Morikawa S, et al. Openings between defective endothelial cells explain tumor vessel leakiness. *Am J Pathol* 2000;156:1363–80.

12. Maeda H. The enhanced permeability and retention (EPR) effect in tumor vasculature: the key role of tumor-selective macromolecular drug targeting. *Adv Enzyme Regul* 2001;41:189–207.
13. Ross D, Kepa JK, Winski SL, et al. NAD(P)H:quinone oxidoreductase 1 (NQO1): chemoprotection, bioactivation, gene regulation and genetic polymorphisms. *Chem Biol Interact* 2000;129:77–97.
14. Cadenas E. Antioxidant and prooxidant functions of DT-diaphorase in quinone metabolism. *Biochem Pharmacol* 1995;49:127–40.
15. Chou TC, Talalay P. Simple generalized equation for analysis of multiple inhibitions of Michaelis–Menten kinetic systems. *J Biol Chem* 1977;252:6438–42.
16. Preusch PC, Siegel D, Gibson NW, Ross D. A note on the inhibition of DT-diaphorase by dicoumarol. *Free Radic Biol Med* 1991;11:77–80.
17. Faig M, Bianchet MA, Winski S, et al. Structure-based development of anticancer drugs: complexes of NAD(P)H:quinone oxidoreductase 1 with chemotherapeutic quinones. *Structure* 2001;9:659–67.
18. Nolan KA, Timson DJ, Stratford IJ, Bryce RA. *In silico* identification and biochemical characterization of novel inhibitors of NQO1. *Bioorg Med Chem Lett* 2006;16:6246–54.
19. Belinsky M, Jaiswal AK. NAD(P)H:quinone oxidoreductase 1 (DT-diaphorase) expression in normal and tumor tissues. *Cancer Metastasis Rev* 1993;12:103–17.
20. Srivastava M, Khurana P, Sugadev R. Lung cancer signature biomarkers: tissue specific semantic similarity based clustering of digital differential display (DDD) data. *BMC Res Notes* 2012;5:617.
21. Awadallah NS, Dehn D, Shah RJ, et al. NQO1 expression in pancreatic cancer and its potential use as a biomarker. *Appl Immunohistochem Mol Morphol* 2008;16:24–31.
22. Siegel D, Franklin WA, Ross D. Immunohistochemical detection of NAD(P)H:quinone oxidoreductase in human lung and lung tumors. *Clin Cancer Res* 1998;4:2065–70.
23. Schlager JJ, Powis G. Cytosolic NAD(P)H:(quinone-acceptor)oxidoreductase in human normal and tumor tissue: effects of cigarette smoking and alcohol. *Int J Cancer* 1990;45:403–9.
24. Lewis AM, Ough M, Hinkhouse MM, et al. Targeting NAD(P)H:quinone oxidoreductase (NQO1) in pancreatic cancer. *Mol Carcinog* 2005;43:215–24.
25. DeNicola GM, Karreth FA, Humpton TJ, et al. Oncogene-induced Nrf2 transcription promotes ROS detoxification and tumorigenesis. *Nature* 2011;475:106–9.
26. Singh A, Misra V, Thimmulappa RK, et al. Dysfunctional KEAP1-NRF2 interaction in non-small-cell lung cancer. *PLoS Med* 2006;3:e420.
27. Cruz FS, Docampo R, Boveris A. Generation of superoxide anions and hydrogen peroxide from beta-lapachone in bacteria. *Antimicrob Agents Chemother* 1978;14:630–3.
28. Boveris A, Docampo R, Turrens JF, Stoppani AO. Effect of beta-lapachone on superoxide anion and hydrogen peroxide production in *Trypanosoma cruzi*. *Biochem J* 1978;175:431–9.
29. Boothman DA, Trask DK, Pardee AB. Inhibition of potentially lethal DNA damage repair in human tumor cells by beta-lapachone, an activator of topoisomerase I. *Cancer Res* 1989;49:605–12.
30. Pink JJ, Planchon SM, Tagliarino C, et al. NAD(P)H:quinone oxidoreductase activity is the principal determinant of beta-lapachone cytotoxicity. *J Biol Chem* 2000;275:5416–24.
31. Planchon SM, Pink JJ, Tagliarino C, et al. Beta-lapachone-induced apoptosis in human prostate cancer cells: involvement of NQO1/xip3. *Exp Cell Res* 2001;267:95–106.
32. Li LS, Bey EA, Dong Y, et al. Modulating endogenous NQO1 levels identifies key regulatory mechanisms of action of beta-lapachone for pancreatic cancer therapy. *Clin Cancer Res* 2011;17:275–85.
33. Docampo R, Cruz FS, Boveris A, et al. Beta-lapachone enhancement of lipid peroxidation and superoxide anion and hydrogen peroxide formation by sarcoma 180 ascites tumor cells. *Biochem Pharmacol* 1979;28:723–8.
34. Imlay JA, Chin SM, Linn S. Toxic DNA damage by hydrogen peroxide through the Fenton reaction *in vivo* and *in vitro*. *Science* 1988;240:640–2.
35. Bentle MS, Reinicke KE, Dong Y, et al. Nonhomologous end joining is essential for cellular resistance to the novel antitumor agent, beta-lapachone. *Cancer Res* 2007;67:6936–45.
36. Haince JF, McDonald D, Rodrigue A, et al. PARP1-dependent kinetics of recruitment of MRE11 and NBS1 proteins to multiple DNA damage sites. *J Biol Chem* 2008;283:1197–208.
37. Beck C, Robert I, Reina-San-Martin B, et al. Poly(ADP-ribose) polymerases in double-strand break repair: focus on PARP1, PARP2 and PARP3. *Exp Cell Res* 2014;329:18–25.
38. Bey EA, Bentle MS, Reinicke KE, et al. An NQO1- and PARP-1-mediated cell death pathway induced in non-small-cell lung cancer cells by beta-lapachone. *Proc Natl Acad Sci USA* 2007;104:11832–7.
39. Tagliarino C, Pink JJ, Dubyak GR, et al. Calcium is a key signaling molecule in beta-lapachone-mediated cell death. *J Biol Chem* 2001;276:19150–9.
40. Pink JJ, Wuerzberger-Davis S, Tagliarino C, et al. Activation of a cysteine protease in MCF-7 and T47D breast cancer cells during beta-lapachone-mediated apoptosis. *Exp Cell Res* 2000;255:144–55.
41. Tagliarino C, Pink JJ, Reinicke KE, et al. Mu-calpain activation in beta-lapachone-mediated apoptosis. *Cancer Biol Ther* 2003;2:141–52.
42. Bey EA, Reinicke KE, Srougi MC, et al. Catalase abrogates beta-lapachone-induced PARP1 hyperactivation-directed programmed necrosis in NQO1-positive breast cancers. *Mol Cancer Ther* 2013;12:2110–20.
43. Park EJ, Min KJ, Lee TJ, et al. Beta-lapachone induces programmed necrosis through the RIP1-PARP-AIF-dependent pathway in human hepatocellular carcinoma SK-Hep1 cells. *Cell Death Dis* 2014;5:e1230.
44. Bentle MS, Reinicke KE, Bey EA, et al. Calcium-dependent modulation of poly(ADP-ribose) polymerase-1 alters cellular metabolism and DNA repair. *J Biol Chem* 2006;281:33684–96.
45. Huang X, Dong Y, Bey EA, et al. An NQO1 substrate with potent antitumor activity that selectively kills by PARP1-induced programmed necrosis. *Cancer Res* 2012;72:3038–47.
46. van Wijk SJ, Hageman GJ. Poly(ADP-ribose) polymerase-1 mediated caspase-independent cell death after ischemia/reperfusion. *Free Radic Biol Med* 2005;39:81–90.
47. Ying W, Sevigny MB, Chen Y, Swanson RA. Poly(ADP-ribose) glycohydrolase mediates oxidative and excitotoxic neuronal death. *Proc Natl Acad Sci USA* 2001;98:12227–32.
48. Woo HJ, Choi YH. Growth inhibition of A549 human lung carcinoma cells by beta-lapachone through induction of apoptosis and inhibition of telomerase activity. *Int J Oncol* 2005;26:1017–23.
49. Park MT, Song MJ, Lee H, et al. Beta-lapachone significantly increases the effect of ionizing radiation to cause mitochondrial apoptosis via JNK activation in cancer cells. *PLoS One* 2011;6:e25976.
50. Szejtli J. Introduction and general overview of cyclodextrin chemistry. *Chem Rev* 1998;98:1743–54.
51. Davis ME, Brewster ME. Cyclodextrin-based pharmaceuticals: past, present and future. *Nat Rev Drug Discov* 2004;3:1023–35.
52. Nasongkla N, Wiedmann A, Bruening A, et al. Enhancement of solubility and bioavailability of β -lapachone using cyclodextrin inclusion complexes. *Pharm Res* 2003;20:1626–33.
53. Hartner PL, Rosen L, Hensley M, et al. Phase 2 dose multi-center, open-label study of ARQ 501, a checkpoint activator, in adult patients with persistent, recurrent or metastatic leiomyosarcoma (LMS). *J Clin Oncol* 2007;25:20521.
54. Torchilin VP, Lukyanov AN, Gao Z, Papahadjopoulos-Sternberg B. Immunomicelles: targeted pharmaceutical carriers for poorly soluble drugs. *Proc Natl Acad Sci USA* 2003;100:6039–44.
55. Jones M-C, Leroux J-C. Polymeric micelles – a new generation of colloidal drug carriers. *Eur J Pharm Biopharm* 1999;48:101–11.
56. Savić R, Luo L, Eisenberg A, Maysinger D. Micellar nanocontainers distribute to defined cytoplasmic organelles. *Science* 2003;300:615–18.
57. Reinicke KE, Bey EA, Bentle MS, et al. Development of beta-lapachone prodrugs for therapy against human cancer cells with

- elevated NAD(P)H:quinone oxidoreductase 1 levels. *Clin Cancer Res* 2005;11:3055-64.
58. Ma X, Huang X, Huang G, et al. Prodrug strategy to achieve lyophilizable, high drug loading micelle formulations through diester derivatives of β -lapachone. *Adv Healthcare Mater* 2014;3: 1210-16.
 59. Rautio J, Kumpulainen H, Heimbach T, et al. Prodrugs: design and clinical applications. *Nat Rev Drug Discov* 2008;7: 255-70.
 60. Perez C, Daniel KB, Cohen SM. Evaluating prodrug strategies for esterase-triggered release of alcohols. *ChemMedChem* 2013;8: 1662-7.
 61. Hooker SC. The constitution of lapachol and its derivatives. Part IV.1 Oxidation with potassium permanganate^{2,3}. *J Am Chem Soc* 1936;58:1168-73.
 62. Xu G, Zhang W, Ma MK, McLeod HL. Human Carboxylesterase 2 is commonly expressed in tumor tissue and is correlated with activation of irinotecan. *Clin Cancer Res* 2002;8:2605-11.
 63. Lu X, Howard MD, Talbert DR, et al. Nanoparticles containing anti-inflammatory agents as chemotherapy adjuvants II: role of plasma esterases in drug release. *AAPS J* 2009;11: 120-2.
 64. Ma X, Huang X, Moore Z, et al. Esterase-activatable β -lapachone prodrug micelles for NQO1-targeted lung cancer therapy. *J Control Release* 2015;200:201-11.
 65. Dong Y, Bey EA, Li L-S, et al. Prostate cancer radiosensitization through poly(ADP-ribose) polymerase-1 hyperactivation. *Cancer Res* 2010;70:8088-96.
 66. Cenas N, Ollinger K. Redox conversions of methemoglobin during redox cycling of quinones and aromatic nitrocompounds. *Arch Biochem Biophys* 1994;315:170-6.
 67. Park HJ, Ahn KJ, Ahn SD, et al. Susceptibility of cancer cells to beta-lapachone is enhanced by ionizing radiation. *Int J Radiat Oncol Biol Phys* 2005;61:212-19.
 68. Reddy S, Li L, Boothman DA, et al. NQO1-mediated synergistic lethality in combination with β -lapachone (β -lap) and ionizing radiation (IR) in head-and-neck cancer (HNC). *Int J Radiat Oncol Biol Phys* 2013;87:S139.
 69. D'Anneo A, Augello G, Santulli A, et al. Paclitaxel and beta-lapachone synergistically induce apoptosis in human retinoblastoma Y79 cells by downregulating the levels of phospho-Akt. *J Cell Physiol* 2010;222:433-43.
 70. Terai K, Dong GZ, Oh ET, et al. Cisplatin enhances the anticancer effect of beta-lapachone by upregulating NQO1. *Anticancer Drugs* 2009;20:901-9.